Electrotransport and Diffusion of Iron and Silver in α-Yttrium

J. E. MURPHY, G. H. ADAMS, AND W. N. CATHEY

The electrotransport mobilities and diffusion coefficients were determined for iron and silver impurities in yttrium. The mobility of iron increased from 1.2×10^{-4} cm^2/V-s at 900°C to 7.4×10^{-4} cm^2/V-s at 1330°C. The silver mobility ranged from 8.1×10^{-6} cm^2/V-s at 905°C to 6.4×10^{-5} cm^2/V-s at 1095°C. The iron movement was anode-directed, and the silver movement was cathode-directed. The diffusion coefficients obtained fit an Arrhenius equation $D = D_0 e^{-\Delta H/RT}$ with the following values:

Fe: $D_0 = 1.8\times10^{-2}$ cm^2/s ΔH = 85 kJ/mol (20 kcal/mol);
Ag: $D_0 = 5.4\times10^{-3}$ cm^2/s ΔH = 77 kJ/mol (18 kcal/mol).

A substitutional-interstitial mechanism previously proposed for anomalously high diffusion rates of impurities in cerium and lanthanum is also proposed for yttrium.

ELECTROTRANSPORT (ET), which is the movement of atoms that occurs when an electric field is applied to a metal, has been reviewed previously.[1-3] Huffine and Williams[4] have demonstrated that electrotransport is a useful technique for purification of yttrium, and the ET of interstitial impurities in yttrium has been investigated by Carlson and others.[5]

The objective of the present work was to study ET and the diffusion of iron and silver impurities in yttrium to supplement work already done in our laboratory on Fe, Co, and Ag in Ce.[6] In cerium, it was observed that the iron and cobalt had very high ET mobilities, and both impurities had diffusion coefficients that were 10^5 times higher than self-diffusion. Silver impurities in cerium did not behave in such a spectacular manner, although the mobilities and diffusion coefficients for silver were considerably higher than would typically be expected from the self-diffusion data. Similar results for diffusion have been reported by Dariel and others[7] for gold and lanthanum in lanthanum. While yttrium is chemically similar to cerium and lanthanum, it has a much higher melting temperature, a different crystal structure, and a significantly smaller ionic radius. Therefore, the data on yttrium should be helpful in furthering the understanding of electrotransport and diffusion in Ce, La, and similar metals.

The relationship between the important parameters in electrotransport is expressed as

$$U = \frac{eZ^*D}{kT} \qquad [1]$$

where e is the electron charge, k is Boltzmann's constant, T is the absolute temperature, D is the uncorrelated diffusion coefficient, Z^* is the effective valence, and U is electrotransport mobility. This study utilized the usual experimental arrangement, which was to apply a constant electric field at temperature T to a bar of metal which contained a non-uniform distribution of the atoms to be studied. The diffusion coefficient was obtained from the change of shape of the distribution, and electrotransport mobility was obtained from the shift in the center of mass of the distribution. By using Eq. [1] and the measured values of U and D, the effective valence, Z^*, was determined.

EXPERIMENTAL PROCEDURES AND RESULTS

The yttrium used for these experiments was prepared by calcium reduction of yttrium fluoride and had a purity of 99+ pct. An analysis of the yttrium is given in Table I.

Some of the yttrium was doped with ^{59}Fe or ^{110}Ag by adding the radioactive material to a well drilled in a 2.5-cm-diam rod, placing a tight-fitting yttrium plug in the well, and arc-melting under purified helium gas. The amount of iron or silver impurity added to the yttrium was so small (< 10 ppm) that the concentration of the impurities was not significantly altered. The resulting cigar-shaped rod was machined to 0.95-cm diam, and discs were then cut from the rod. The discs were surface-ground to just over the desired thickness and subsequently lap-polished to a final 0.127-cm thickness. A disc was then placed between two rods of pure yttrium, each 0.95 cm in diam and 5 cm in length, and

Table I. Analysis Yttrium Metal†

Impurity Element‡	Wt Pct
Aluminum	0.007
Copper	0.004
Iron	0.01
Nickel	0.013
Silicon	0.01
Zirconium	0.5
Carbon	0.04
Oxygen	0.35

†Metallic impurities were determined by atomic absorption and emission spectrography analyses. Oxygen was determined by inert gas fusion and carbon by combustion.

‡All other impurities were less than 0.001 wt pct or were below the limits of detection.

J. E. MURPHY is a Physicist at the Reno Metallurgy Research Center, Bureau of Mines, U.S. Department of the Interior, Reno, Nevada, 89505. G. H. ADAMS is a former Physical Science Aide with the Bureau of Mines, Reno, Nevada. W. N. CATHEY is Research Physicist at the Reno Metallurgy Research Center, and is Associate Professor of Physics, University of Nevada, Reno, Nevada.

Manuscript submitted April 3, 1974.

the resulting sandwich was clamped in a water-cooled welding jig. After evacuating to 5×10^{-6} torr, the disc was welded to the rods by passing 600 A through the rods for 25 s. This procedure resulted in strong, uniform welds. Analysis of a rod welded in this manner showed that negligible diffusion occurred during welding.

After welding, the ends of the rod were tapped 3 cm deep for a 12-24 thread, and two molybdenum rods, each 0.5 cm in diam by 10 cm long, were screwed into the ends. The yttrium sample and the molybdenum connecting rods are shown in Fig. 1. The lower molybdenum rod was threaded into a circular, 1.3-cm-thick, water-cooled copper plate, which was grounded and served as the cathode. The upper molybdenum rod was attached to a 2.54-cm copper rod which was connected to the anodic side of the rectifier by electrical feedthroughs. Both molybdenum rods were reduced to 0.32-cm diam for 1.3 cm of length near the end that was inserted into the yttrium. As a result, the molybdenum electrodes heated to a higher temperature than the yttrium rod during the experiments. Under these conditions the thermal gradient was reduced to less than 5°C over the 10-cm-long yttrium sample.

A heater element, 2.5 cm in diam by 23 cm long, made from 0.0025-cm-thick tantalum foil, surrounded the yttrium rod. The purpose of the heater was to minimize radial temperature gradients in the yttrium sample. The lower end of the element was clamped to the water-cooled copper plate which served as an electrical ground, and the upper end was clamped to a copper rod which was insulated from the molybdenum electrode by a boron nitride spacer. The copper rod was connected to a stabilized transformer which powered the heating element, and three small holes were punched in the heater to allow observation of the yttrium rod. A water-cooled copper jacket was placed around the heater to prevent unnecessary heating of the vacuum chamber during an experiment. Holes in the copper jacket lined up with the observation holes in the heater element.

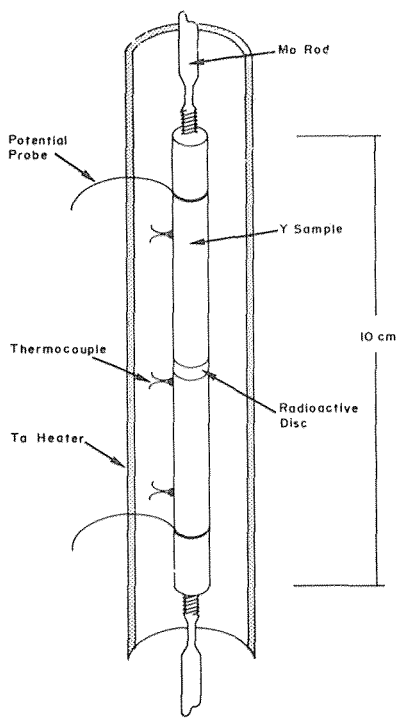

Fig. 1—Yttrium sample in copper holder.

For the ET experiments with the iron impurity, the direct current passing through the yttrium sample was held constant at 100 A. The corresponding current density was 140 A/cm^2, and the field intensity averaged about 0.025 V/cm. The field intensities which were necessary to determine the ET mobilities were determined from potential drop measurements made with the molybdenum wire potential probes shown in Fig. 1. The values were checked by calculating the field intensities from the current, sample diameter, and the resistivity.[8] In these experiments, the sample temperature was varied by controlling the heater temperature. With the silver impurity, the vapor pressure was sufficiently high that a significant percentage of the silver vaporized. The vaporized Ag was restricted from moving away from the yttrium by the tantalum element. As a result, the silver was continually vaporizing from and redepositing on the surface of the yttrium, thus giving rise to erroneous diffusion coefficients. To eliminate this problem, and to obtain the maximum ET movement before too much silver vaporized, the tantalum heater was removed during the Ag-ET experiments. Hence, in the silver experiments, all heating was from the direct current. In this case, the current densities ranged from 300 A/cm^2 to 500 A/cm^2 and the corresponding field intensities were from 0.05 V/cm to 0.1 V/cm. Even with the heater removed, the experiments with silver could not be performed above 1200°C because the vaporization became intolerable.

As stated previously, the purpose of the heater was to minimize radial temperature gradients. To determine the radial temperature gradient, a calculation was made following an analysis given by Kreith.[9] The calculated gradient was found to be about 15°C from the center to the surface of the sample at 1100°C. In the silver experiments, the radial thermal gradient was taken into account by calculating an average sample temperature.

The direct current for all ET experiments was supplied by a Hewlett-Packard* model 6466A power supply, the output of which is well regulated and has very little drift.

*Reference to specific brands is made for identification only and does not imply endorsement by the Bureau of Mines.

In addition to the ET experiments, several separate diffusion experiments were made with both iron and silver impurities. In these experiments, the apparatus shown in Fig. 2 was used. The yttrium rod was held at room temperature in the baffled compartment until the resistance furnace reached the desired temperature. The sample was then lowered into the hot zone, and heated rapidly to the operating temperature in a purified helium atmosphere. With this apparatus thermal gradients were essentially nonexistent and control of the temperature was excellent. The results of these experiments agreed closely with the data obtained from the ET experiments.

The temperature of the rod during the ET experiments was measured by means of an optical pyrometer. A correction for absorption by the glass bell jar was applied to the recorded temperature. No emissiv-

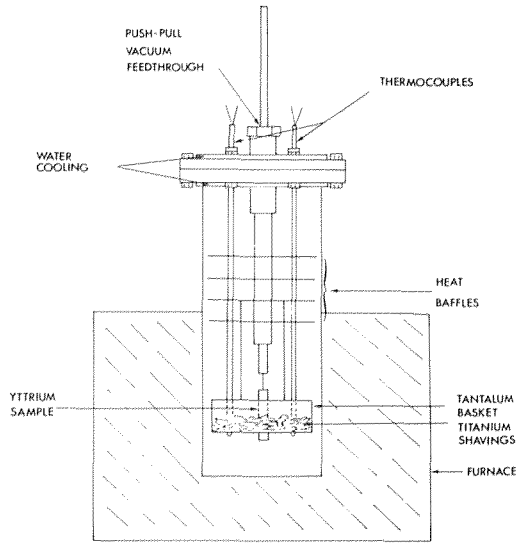

Fig. 2—Apparatus for separate diffusion experiments.

ity corrections were made because the machined surface was relatively rough, and it oxidized during initial heating. In addition, the diffusion data obtained from the separate experiments agreed reasonably well with the data from the ET experiments. Likewise, a comparison of measured field intensities checked closely with the field intensities calculated from the resistivity data. With the iron impurity experiments, the tantalum element was about 100°C less than the sample temperature, and thus, nearly black body conditions existed for the pyrometer readings. A movable baffle protected the bell jar enclosure from deposition of vaporized material except when pyrometer sightings were being made. In addition, the temperature was monitored by three Chromel-Alumel thermocouples when the experimental temperature was below 1200°C. The thermocouples projected through the lower copper plate and were spot-welded to the yttrium rod. The thermocouple outputs were recorded on a multipoint chart recorder. Because of the method of attaching the thermocouple, the thermocouple temperatures were usually about 50°C lower than the optical reading, and therefore, the temperature of the rod was adjusted by the optical readings. However, the thermocouples made temperature monitoring convenient and gave a good indication of the temperature gradient along the sample.

Following an electrotransport experiment, the radioactivity in the rod was surveyed by monitoring 1.27-cm segments using a scintillation counter apparatus described previously.[6] This survey was used to determine what portion of the rod had to be sampled. Excess material was removed from the ends of the rod, and careful measurements were made of the distance from the ends of the rod to the disc by a traveling microscope which was accurate to 0.001 mm. The rod was placed in a precision lathe and the surface removed to minimize surface diffusion effects. Then the sample was machined in 0.127-cm segments along the length.

The apparatus shown in Fig. 3 was developed to collect the shavings taken from the sample by the lathe. The sample was partly surrounded by a small hood which was connected by a rubber hose to a cyclone-

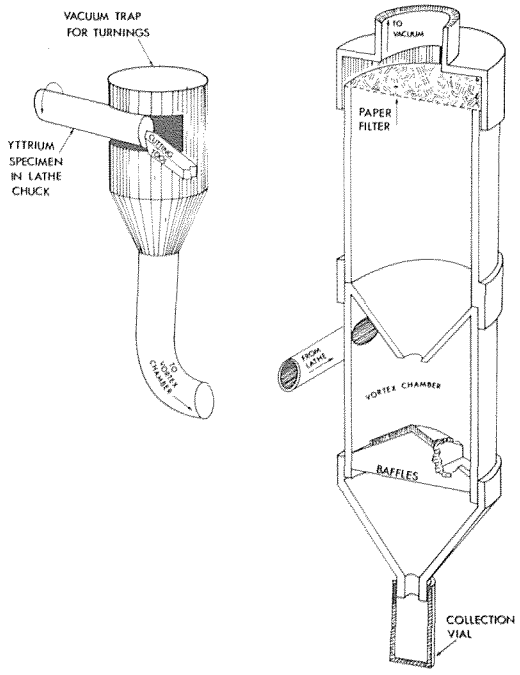

Fig. 3—Sampling apparatus.

type chamber. The shavings were drawn by a vacuum into the chamber where they spiraled down the sides until caught by fins on the baffle, which caused them to fall into the collection vial. If any shavings did get carried toward the vacuum, they were trapped on a filter. After 0.127 cm of the sample had been removed, the vacuum was shut off, and the chamber side tapped to insure any shavings on the filter fell to the collection vial. This collection system proved to be very satisfactory, and the samples obtained were so uniform that weighing was found to be unnecessary.

The samples were analyzed in a deep well scintillation counter adjusted to count the γ-ray energy of the impurity of interest. A typical plot of the data is shown in Fig. 4. The displacement, as a result of ET, was measured by finding the center of the impurity profile after the experiment and comparing it with the center of the disc. The center of the impurity profile was the position that divided the radiotracer counts into two equal parts. The diffusion coefficient was obtained from the experimental results by a computer fit of the data to the solution given by Jost for diffusion out of a disc:[10]

$$C(x) = \frac{C_0}{2}\left[\operatorname{erf}\left(\frac{h+x}{2\sqrt{Dt}}\right) + \operatorname{erf}\left(\frac{h-x}{2\sqrt{Dt}}\right)\right], \qquad [2]$$

where h is one-half the width of the disc, C_0 is the original concentration of radioactive impurity (obtained by adding the count rates for each segment and correcting for background radiation), and $C(x)$ is the concentration at distance x from the center of the disc at time t for the diffusion coefficient D.

The experimental results are given in Table II. The ET mobilities shown are very high compared to typical values for substitutional impurities as given by Verhoeven.[11] The mobilities are also plotted as a function of temperature in Fig. 5. The uncertainties in the ET mobilities as given in Table II are an estimate of the

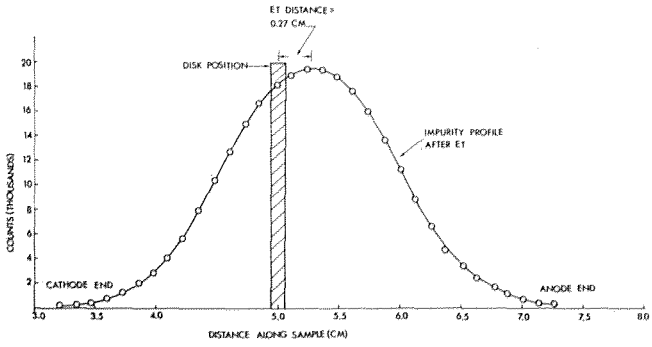

Fig. 4—Typical plot of data from an electrotransport and diffusion experiment with ^{59}Fe in Y.

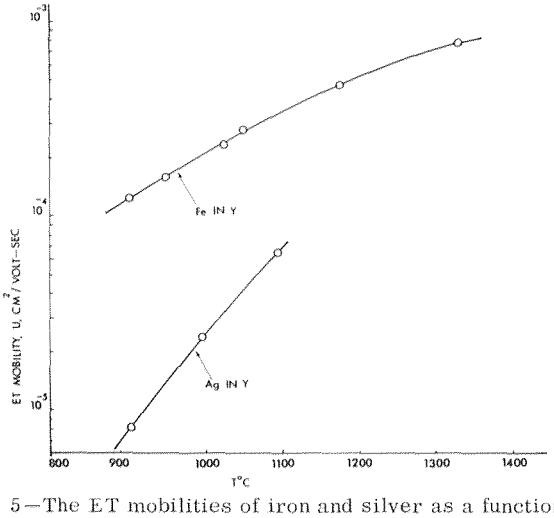

Fig. 5—The ET mobilities of iron and silver as a function of temperature.

errors encountered in the measurements. The major sources of error included temperature variations, distortion of the disc during welding, statistical error in the radiotracer counts, variations in the mass of the shavings, and errors in machining the samples. In a few cases, duplicate experiments were made and the U values were reproducible within the quoted error limits.

Table II also shows the diffusion coefficients which are very high compared with typical substitutional impurity diffusion or compared with self-diffusion in yttrium as determined by Gorny and Altovskii.[12] The separate diffusion experiments gave more accurate data, primarily because the temperature could be more closely controlled. The errors listed in Table II for the diffusion coefficients are conservative estimates based on the precision of the computer fit of the experimental data and on the possible errors in temperatures.

The diffusion coefficients are plotted as a function of $1/T$ °K in Fig. 6. A least squares computer program was used to obtain the best plot of the data. The program was also used to calculate the frequency factors, D_0, and the activation energies, ΔH, for the Arrhenius equation,

$$D = D_0 e^{-\Delta H/RT} \qquad [3]$$

The frequency factors and activation energies and their uncertainties as determined from the least square analysis are shown in Table III.

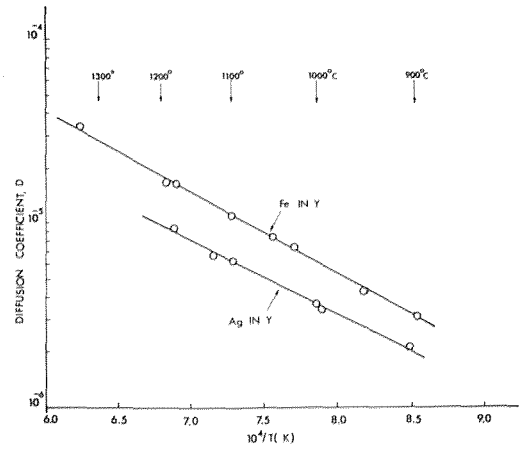

Fig. 6—The diffusion coefficients of iron and silver as a function of temperature.

Table II. Electrotransport and Diffusion Experimental Data

Impurity	T (°C)	U (cm²/v-s)	D (cm²/s)	Z^*
Fe	900 ± 10	(1.2 ± 0.5) × 10^{-4}	(3.2 ± 0.3) × 10^{-6}	−3.8 ± 2
	950 ± 10	(1.6 ± 0.3) × 10^{-4}	(4.1 ± 0.3) × 10^{-6}	−4.1 ± 1
	1025 ± 10	(2.3 ± 0.3) × 10^{-4}	(7.5 ± 0.5) × 10^{-6}	−3.4 ± 1
	1050 ± 10	(2.8 ± 0.3) × 10^{-4}	(8.4 ± 0.2) × 10^{-6}	−3.8 ± 0.5
	1100 ± 5	†	(1.09 ± 0.2) × 10^{-5}	—
	1175 ± 10	(4.6 ± 0.4) × 10^{-4}	(1.60 ± 0.2) × 10^{-5}	−3.6 ± 1
	1190 ± 5		(1.63 ± 0.2) × 10^{-5}	—
	1330 ± 10	(7.4 ± 0.3) × 10^{-4}	(3.28 ± 0.3) × 10^{-5}	−3.1 ± 0.5
Ag	905 ± 20	(8.1 ± 0.4) × 10^{-6}	(2.1 ± 0.4) × 10^{-6}	+0.4 ± 0.2
	995 ± 20	(2.3 ± 0.3) × 10^{-5}	(3.3 ± 0.5) × 10^{-6}	+0.8 ± 0.2
	1000 ± 5		(3.6 ± 0.3) × 10^{-6}	—
	1095 ± 20	(6.4 ± 0.3) × 10^{-5}	(6.2 ± 0.5) × 10^{-6}	+1.2 ± 0.2
	1125 ± 5		(6.7 ± 0.3) × 10^{-6}	—
	1180 ± 5		(9.3 ± 0.3) × 10^{-6}	—

†Diffusion experiment only.

Table III. Frequency Factors and Activation Energies for Fe and Ag in Y

Impurity	D_0, (cm²/s)	ΔH, kJ/mol (kcal/mol)
Fe	(1.8 ± 0.1) × 10^{-2}	85 ± 2 (20)
Ag	(5.4 ± 0.3) × 10^{-3}	77 ± 4 (18)

The Z^* values in Table II were calculated from the mobilities and diffusion coefficients using Eq. [1]. The errors associated with Z^* are large because they combine the uncertainties in D and U. The Z^* values are typical for ET in solid metals.

The experimental data shown in Table II indicate that ET would be a practical purification technique with respect to the iron and silver impurities. Two ET experiments were made with yttrium samples containing 2 wt pct iron to clearly demonstrate the degree of purification that could be expected. The yttrium samples were prepared by adding iron powder to yttrium metal and arc-melting several times to insure homogeneity. The samples were machined to rods, 0.95 cm in diam by 10 cm long. The tantalum heater in the apparatus was eliminated to obtain the highest possible field intensity. Other details of the experiments were the same as those previously described.

One experiment was performed at 975°C for 50 h with

a field intensity of 0.06 V/cm and a current density of 325 A/cm^2. The other experiment was made at 1200°C for 60 h with a field intensity of 0.1 V/cm and a current density of 500 A/cm^2. Following the ET, the samples were divided into 1-cm segments, and the segments were analyzed for iron content. The lower limit of detection for the analysis was 0.01 wt pct iron. The results of the experiments are plotted in Fig. 7 and show that considerable purification has taken place in both samples. More purification is shown by the sample that was run at 1200°C.

DISCUSSION

The values for ET mobilities and diffusion coefficients obtained for iron and silver in yttrium are very high for substitutional impurities in solid metals. Similar results were found for iron and cobalt in cerium, but the ET mobilities and diffusion coefficients for silver in cerium were much lower.[6]

In view of Eq. [1] the high ET mobilities were due to the high diffusivities rather than any unusually high Z^* values. It is also evident that the success of ET for the purification of yttrium with respect to iron is primarily due to the high diffusion rate of iron. Verhoeven[11] noted that only in those systems exhibiting anomalously high diffusion coefficients would ET purification be practical, and from the limited data currently available, it appears that anomalously high diffusion coefficients are relatively common for metallic impurities in the rare-earth metals. Thus ET appears to be a promising purification technique for these metals.

Probably the most interesting result of the present work, from the fundamental point of view, is the discovery of another system in which metal impurities in a host metal diffuse many orders of magnitude faster than the host metal atoms. This was observed many years ago for gold in lead,[13] but only recently has ultra-fast diffusion become of interest because of the possible metallurgical effects and because of considerable theoretical interest in the mechanism by which such diffusion occurs.[14]

Table IV provides a comparison of impurity diffusion and self-diffusion in yttrium and cerium at 0.8 of the melting temperature of each host. Diffusion activation energies are also listed. It should be noted that the diffusion coefficients obtained for iron and silver impurities in yttrium are approximately 10^5 times higher than the self-diffusion data by Gorny and Altovskii.[12] Clearly iron and silver in yttrium represent a case of ultra-fast diffusion similar to Fe and Co in Ce. A substitutional-interstitial mechanism previously developed[16] for explaining ultra-fast diffusion assumes that some of the impurities are in substitutional lattice sites while others are in interstitial sites. Those impurities in interstitial sites normally diffuse more rapidly because adjacent interstitial sites are readily available into which an impurity can move. On the other hand, substitutional diffusion normally occurs only when a vacancy is available with an impurity can exchange. Since interstitial diffusion is many orders of magnitude faster than substitutional diffusion, even a small fraction of impurities in interstitial sites can give rise to a large increase in net impurity diffusion.

It was suggested in an earlier paper[6] that iron and cobalt diffused in cerium mainly as interstitials, while only some small fraction of the silver present was diffusing interstitially. In order to compare the cerium data with the similar results for impurity diffusion in lanthanum by Dariel and others,[15] some size arguments were made. The radius of the largest hard sphere which can fit into the octahedral interstitial site defined by the ion cores of the host metal is given by $R - r_H$, where R is the distance of closest approach for the host ions and r_H is the radius of the host ion. If those same size arguments are made for yttrium, the radius of the largest hard sphere which fits into the octahedral interstitial hole in the hcp yttrium lattice is found to be 1.63×10^{-10} m (using the ionic radius of Y^{+3} as 0.93×10^{-10} m), compared with 1.43×10^{-10} m for the octahedral hole in fcc cerium. The larger hole size in yttrium may allow a larger fraction of silver into the interstitial sites in yttrium than in cerium. This would explain the fact that silver as well as iron diffuses very rapidly in yttrium, whereas the diffusion of silver in cerium is three orders of magnitude slower than iron in cerium. Thus, the data for yttrium are consistent with the model developed for Ce. However, it must be

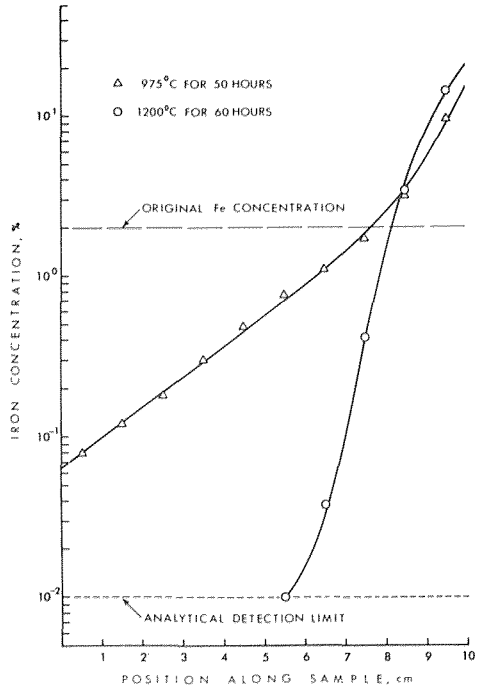

Fig. 7—Purification of yttrium samples containing 2 pct iron.

Table IV. Comparison of Diffusion Data

System	Ref.	D at 0.8 T_M, (cm^2/s)	0.8 T_M, (°C)	Activation Energy, kJ/mol (kcal/mol)
Y in Y (Single crystal)	12			
a axis		2.5×10^{-10}	1153	281 (67.1)
c axis		4.4×10^{-10}		252 (60.3)
Ag in Y		8.0×10^{-6}		77 (20)
Fe in Y		1.4×10^{-5}		85 (18)
Ce in Ce	15	2.8×10^{-10}	602	153 (36.6)
Ag in Ce	6	2.3×10^{-8}		117 (28)
Co in Ce	6	1.6×10^{-5}		46 (11)
Fe in Ce	6	2.1×10^{-5}		19 (4.6)

emphasized that these crude size arguments can provide only rough guidelines for the existence of significant fractions of impurities in interstitial sites. A complete description must include the electronic interactions, but unfortunately, no general theory is available at this time.

It should be mentioned that the diffusion coefficients of C, O, and N in yttrium determined by Carlson and others[5] were very close to the values of D for iron and silver in yttrium at the same temperature. This further supports the hypothesis that iron and silver diffusion in yttrium is dominated by an interstitial mechanism, since C, O, and N are interstitial impurities.

In metals, the ET force which causes the movement of impurities is thought to be due mainly to the momentum transfer from the current-carrying electrons as they are scattered by the atoms in the metal. Various models were reviewed by Verhoeven.[1] The actual average ET force is given by eZ^*E; however, results are usually quoted in terms of the effective valence, Z^*. The sign of Z^* indicates the direction the impurity moves, and from Table II it is seen that iron goes toward the anode while silver moves to the cathode.

The direction of the ET can be explained in terms of the electronic band structure of the yttrium. Huntington and Ho[17] have discussed the fact that electron-like current carriers give a force toward the anode while hole-like current carriers give a force toward the cathode. The band structure of yttrium, according to Gschneidner,[18] consists of two bands: a nearly full 5s band which is hole-like at the Fermi surface, and an electron-like 4d band containing about one electron per atom. Obviously the momentum transfer toward the anode from the 4d band to the iron impurity, and also to the anode-directed C, O, N, and H impurities[5] is greater than the momentum transfer toward the cathode from the 5s band. The opposite is true for silver. In view of the different electronic structure of the iron and silver impurities, the observed differences in net ET force are not surprising, and it is concluded that any prediction of the ET direction would require detailed knowledge of the impurity and the host-metal band structure in the case of multiband metals. Average properties such as the Hall coefficient are of limited value for predicting the ET direction in multiband metals as emphasized by the fact that iron and silver behave similarly in yttrium and cerium, yet the Hall coefficient is negative for yttrium and positive for γ-cerium.[18]

While this model reconciles different directions of ET in a multiband metal such as yttrium, it will require detailed theoretical analysis for confirmation.

CONCLUSIONS

The rapid diffusion observed for iron and silver in yttrium can be explained in terms of a substitution-interstitial mechanism. This rapid diffusion was responsible for the considerable purification of yttrium with respect to iron by the method of electrotransport.

ACKNOWLEDGMENTS

The authors wish to thank T. A. Henrie and M. M. Wong for their assistance with the project.

REFERENCES

1. J. D. Verhoeven: *Met. Rev.*, 1963, vol. 8, p. 311.
2. D. T. Peterson: *Atomic Transport in Solids and Liquids*, Verlag der Zeitschrift für Natürforschung, p. 104, Tübingen, 1971.
3. H. B. Huntington: *Trans. TMS-AIME*, 1969, vol. 245, p. 2571.
4. C. L. Huffine and J. M. Williams: *The Rare Earths*, 1961, ch. 11, p. 156.
5. O. N. Carlson, F. A. Schmidt, and D. T. Peterson: *J. Less-Common Metals*, 1966, vol. 10, p. 1.
6. W. N. Cathey, J. E. Murphy, and J. R. Woodyard: *Met. Trans.*, 1973, vol. 4, p. 1463.
7. M. P. Dariel, G. Erez, and G. M. J. Schmidt: *Phil. Mag.*, 1969, vol. 19, p. 1053.
8. C. E. Habermann and A. H. Daane: *J. Less-Common Metals*, 1963, vol. 5, p. 134.
9. F. Kreith: *Principles of Heat Transfer*, 2nd ed., pp. 45-46, International Textbook Co., Scranton, Pa., 1969.
10. W. Jost: *Diffusion in Solids, Liquids, Gases*, p. 23, Academic Press, N.Y., 1960.
11. J. D. Verhoeven: *J. Metals*, 1966, vol. 18, p. 26.
12. D. S. Gorny and R. M. Altovskii: *Diffusion Data*, 1970, vol. 4, p. 456.
13. W. Seith and T. Heuman: *Diffusion in Metal*, Springer-Verlag, 1955.
14. N. L. Peterson: *Solid State Phys.*, Seitz and Turnbull, eds., 1968, vol. 22, p. 444.
15. M. P. Dariel, G. Erez, and G. M. J. Schmidt: *Phil. Mag.*, 1969, vol. 19, p. 1053.
16. G. V. Kidson: *Phil. Mag.*, 1966, vol. 13, p. 247.
17. H. B. Huntington, and S. C. Ho: *J. Phys. Soc. Japan*, 1963, vol. 18, Suppl. II, p. 202.
18. K. A. Gschneidner, Jr.: *Proceedings of the Fourth Conference on Rare Earth Research*, L. Eyring, ed., p. 153, Gordon and Breach, N.Y., 1965.